Proc. Of the 3rd International E-Conference on Advances in Engineering, Technology and Management - ICETM 2020

ISBN: 978-1-63248-190-0 DOI: 10.15224/978-1-63248-190-0-13

Speckle Denoising in Images Using 3D Filter Based on Maximum a Posteriori Probability Estimator

G. Aranda-Bojorges, V. Ponomaryov, R. Reyes-Reyes
Instituto Politecnico Nacional, Mexico-city

Abstract*— Image denoising is considered as an effective initial processing step in different sophisticated imaging applications. Over the years, numerous studies have been conducted filtering of different kinds of noise. The Block Matching with 3D filtering added a new dimension to the study of denoising techniques. The main motive of this work is to establish a novel denoising method for multiplicative noise (speckle), with the ideology of the sparse representation in filtering via Maximum a Posteriori (MAP) estimator approach that is used in 3D array performed by grouping similar patches. Experimental results justified a good performance of novel framework that appears to demonstrate better denoising performance against state-of-art algorithms according objective criteria (PSNR, SSIM, EPI) values as well as subjective visual perception. *(Abstract)

Keywords—Denoising, 3D filtering, MAP estimator.

I. Introduction

Despeckling filters aim at estimating the noise-free image of fan acquisition system. To describe denoising methods that have been developed, the speckle model should be defined. Synthetic Aperture Radar (SAR) and Ultrasound (US) are some examples from active acquisition sensors that produce a radiation and capture the signal backscattered from an area of interest in the imaging scene (resolution cell). If we assume that the resolution cell contains several scatters and there are no anyone that yields a reflected signal *P* much stronger than others, the received signal can be viewed as the incoherent sum of several backscattered waves, i.e., $Ae^{j\phi} = \sum_i A_i e^{j\phi_i}$. The amplitudes A_i and phases ϕ_i are the results of several factors, including propagation attenuation, scattering of the illuminated targets. Even if the underlying reflectivity field is uniform, it can be affected by a granular noise in an imaging registered. The phases ϕ_i are highly varying, the usually are considered as uniformly distributed ones in $(-\pi, \pi)$ as well as independent of A_i, which its probability density function (pdf) is described by Rayleigh pdf:

$$P_A(A) = \frac{A}{\sigma^2}\exp\left(-\frac{A^2}{2\sigma^2}\right),$$

and the power or intensity $I = A^2$ is distributed according to an exponential pdf, that is: (1)

$$P_I(I) = \frac{1}{\sigma}\exp\left(-\frac{1}{\sigma}\right). \quad (2)$$

In other cases, the result may be approximated as Gamma distribution: (3)

$$P_I(I) = \frac{L^L I^{L-1} e^{-LI}}{\Gamma(L)},$$

where $I \geq 0$, $\Gamma(L)$ denotes the Gamma function and L is the equivalent number of looks. Considering the image I and a multiplicative noise R as independent random variables, we can obtain (4)

$$P_{I|R}(I|R) = P_I\left(\frac{I}{R}\right)\frac{1}{R} = \frac{L^L I^{L-1}}{\Gamma(L)R^L}\exp\left(-\frac{LI}{R}\right). \quad (5)$$

The most used model in the literature on Despeckling is the following multiplicative one:

$$i = nx,$$

where x is a random process and represents the noise-free image, n is a speckle noise that is modeled as a random process and it is independent of x; finally, i is the observed noisy image. The non-linear nature of the relationship between the observed and the noise-free signals makes the filtering procedure a non-trivial task. For this reason, some transformations could be introduced to apply effective (6) mathematical techniques. Several authors accept the following model, derived from (5):

$$i = n + n(x-1) = x + v,$$

where $v = n(x-1)$ accounts for speckle disturbance in an equivalent additive model, in which, v depending on n, is a signal dependent noise process.

Another approach that allows the multiplicative noise to be transformed into additive one consists the usage of a homomorphic transformation [1]. This technique employs the logarithm operation of the observed images. In the most studies, approaches to image denoising that perform estimation in a transformed domain have been perform proposed. Transforms derived from multiresolution signal analysis [2, 3], such as the discrete wavelet transform (DWT), are the most popular in this context. Despeckling in a transform domain should be carried out by taking the direct transform of the observed signal and estimation of speckle-free coefficients following by reconstruction in the filtered image through the invers transform applied to the despeckled coefficients,

Proc. Of the 3rd International E-Conference on Advances in Engineering, Technology and Management - ICETM 2020

ISBN: 978-1-63248-190-0 DOI: 10.15224/978-1-63248-190-0-13

II. Related Work

The presence of speckle noise can greatly deteriorate the quality of images, in particular, fine details and edges that are important features in different image processing applications, such as classifications, detection, artificial viewing, pattern recognition, etc. Thus, despeckling is a major requirement to reduce the risk due to wrong interpretation in SAR or US images. Numerous studies in techniques of denoising in images can be categorized into five principal classes:

- Adaptive filters. These filters are based on the idea of assigning weighting coefficients for pixels in each window whose characteristics are based on local statistical properties. It is supposed that they do not alter much the edges or fine details in an image much. The frequently used adaptive filters include median filters [4], bilateral filters, [5], and SRBF filter [6], which perform under the assumption that the speckle noise has a multiplicative nature. These filters tend to blur the image though the can be characterized by low computational complexity; therefore, sometimes the have a better speckle suppression than edge preservation and vice versa [7].
- Anisotropic diffusion filters. These filters include the SRAD [8], DTD [9], and OSRAD [10] filters. They demonstrate to have a good speckle reduction capability, but they can over-smooth the fine details and edges, resulting in a very low edge preservation performance.
- Non-local means filters. These techniques constitute the recently designed despeckling algorithms, such as OBNLM [11], Lee filter [12], etc., demonstrating a good speckle suppression but high computational complexity. Since the denoising in the remote sensing and medical imaging are the operations in real time usually, their complexity could be a serious drawback in applications.
- Multi-scale methods. Numerous studies in despeckling use multi-scale analysis due to their advantages of temporal-frequency methods and a low computational complexity. These techniques include some classical works, such as Donoho's soft thresholding [13] and Andria filter [14].
- BM3D type techniques. These techniques are based on forming groups of different patches, according to chosen reference patch. These patches should be grouped in order to perform 3D arrays of different segments in an image. The arrays are used for the purpose of filtering procedure applied because their low computational complexity and the high performance in the det ails preservations [15].

A great deal of study regarding to speckle modeling has been done by Insana et al. [16], but they considered only speckle at the transducer of the acquisition system. Godman et al. [17] performed a study in describing speckle in laser images and have evaluated the speckle modeling via Rayleigh pdf. This approach has been used by Burckhardt et al. [18], where they ascertained this distribution. This also satisfied with narrow band speckle. Wagner et al. [19] has employed the Racian pdf in modeling the speckle noise. Jakeman et al. [20] considered a weak scattering model and they assumed that the pdf can be presented by K-distribution. This was supported by Wang et al. [21].

Resuming this brief review of existing techniques in despeckling, we can conclude that most of them cannot guarantee a balanced performance between speckle reduction and edge preservation that are the principal performance characteristics in different application where these images can be used.

III. Proposed Method

The following subsections describe the detailed explications of the proposed denoising scheme.

1) Logarithmic Transformation

Let first consider an image affected by speckle noise, as described in (5), so it is necessary to perform the logarithmic transformation, such as:

$$e = \log(i) = \log(nx) = \log(n) + \log(x), \tag{7}$$

$$e = f + \eta, \tag{8}$$

where e, f and η are the logarithmic transformation of i, n and x, respectively. Hence, the transformed speckle coefficient is reduced to:

$$\eta = e - f \tag{9}$$

2) Segmentation

To establish the number of references patches within an image, it is necessary to perform the histogram and, considering its number of peaks, we can use it to determine the number of reference patches. Then, we use k-means segmentation and, for this, first, the centroids should be randomly selected. This procedure iterates until the centroids have any changes. Resulting in the centroids of every patch of reference chosen, which is the size 5×5, the similar patches are associated by Euclidian distance, where the lower value is, the more similar are. Finally, we can perform the grouping of the 3D arrays.

3) Evaluation of Patch Correlation

The next step is to determine the level of correlation between the patches in the 3D arrays. The study of a noise in images is not confined to a small point but extends over a large area.

Proc. Of the 3rd International E-Conference on Advances in Engineering, Technology and Management - ICETM 2020

ISBN: 978-1-63248-190-0 DOI: 10.15224/978-1-63248-190-0-13

Hence, it is necessary the correlation properties of the speckle noise. The aim is to evaluate the correlation properties according to the adjacent patches and their variations when the number of patches is increased . So, it is necessary to extract the speckle coefficients from the image.

In (9), e denotes the set of the logarithmic transformations of all the N patches i.e. $\boldsymbol{e} = [e_1, e_2, \dots, e_n]$ and each $e_i = \log(i_j)$. The problem consists of finding the noise free image x as mentioned in (7). Let consider N patches of a 3D block that are extracted the invariant regions using background extraction methods and averaged it to get a single image finally estimating the noise free image, $x = \text{mean}(i_1, i_2, \dots, i_n)$.

To determine the correlation, let us consider two patches of size $P \times Q$, so, the correlation between two patches, $\boldsymbol{X}$ and $\boldsymbol{Y}$, denoted by $C_{X,Y}$, is calculated by finding the correlation between the same speckle coefficients of these two patches as follows:

$$C_{X,Y} = \frac{1}{(P-1)(Q-1)} \sum_{j=1}^{Q-1} \sum_{k=1}^{P-1} \frac{E[X_{j,k} - \mu_X] E[Y_{j,k} - \mu_X]}{\sigma_X \times \sigma_Y} \quad (10)$$

Here, μ_X and σ_X denote the mean and the variance of speckle coefficients of $\boldsymbol{X}$, respectively. Similarly, μ_Y and σ_Y denote the mean and the variance of speckle coefficients of $\boldsymbol{Y}$, respectively. The process can be repeated for $\boldsymbol{N}$ patches. This correlation can be effectively utilized for estimating the noise-free pixels in the noisy data.

4) Estimation of Noise-Free Pixels

Using the correlation between different patches of an image, we can estimate a denoised image. We propose to replace the noisy pixels by their MAP estimation, considering the pixels modelled by multivariate Gaussian distribution. The idea has been exploited by Tian et al. [22], where there has been assumed that the pixels belong to univariate Gaussian distribution. The fundamental difference in the designed framework that we consider an image for the purpose of denoising. The MAP estimation of a single pixel is obtained by considering the same pixel of all the $\boldsymbol{N}$ patches along with the correlation between these pixels, as mentioned previously, to get a single denoised image. The MAP estimate of the noisy pixel is given by following:

$$\hat{n} = \underbrace{\max}\,(p(m|n)). \quad (11)$$

Using Bayes rule, (11) can be written as:

$$p(n|m) \propto p(m|n)p(n). \quad (12)$$

Our aim is to model the two density probably functions $p(m|n)$ and $p(n)$. The logarithmic transformed data $p(m|n)$ is assumed to be Gaussian pdf, as used in different studies, such as [23]. So, the model for data can be written as follows:

$$p(m|n) = \frac{1}{\sqrt[n]{2\pi}} \frac{1}{\sqrt{|K|}} \exp\left(-\frac{1}{2}(m - nA)^T \|K\|^{-1}(- - nA)\right). \quad (13)$$

It should be noted that m is the vector of all noisy pixel values from the $\boldsymbol{N}$ consecutive patches, and n us the noise-free value of the corresponding pixels. A represents unity vector and R is the covariance matrix, which can be extracted from the $\boldsymbol{N}$ patches. Let consider two patches of the size $P \times Q$; the covariance between two patches e_X and e_Y, denoted by Σ_{e_X,e_Y} is calculated by:

$$\Sigma_{e_X,e_Y} = \frac{1}{PQ} \sum_{j=1}^{Q-1} \sum_{k=1}^{P-1} E\left[e_{X_{j,k}} - \mu_{e_X}\right] E\left[e_{Y_{j,k}} - \mu_{e_Y}\right],$$

where μ_{e_X} and μ_{e_Y} denote the mean of speckle coefficients on patch n_X and n_Y, respectively.

The priori term $p(n)$ is assumed to be Gaussian, with $\bar{m}$ as the mean of the set of noisy pixels from the 3D array, corresponding to each noise-free pixel and σ as the standard deviation of the same.

$$p(n) = \frac{1}{\sqrt{2\pi}\sigma} \exp\left(-\frac{(n-\bar{m})}{2\sigma^2}\right). \quad (15)$$

Substituting (13) and (15) in (12), we get

$$p(n|m) \propto \frac{1}{\sqrt{2\pi|\Sigma|}} \exp\left(-\frac{1}{2}(m - nA)^{T\Sigma^T}(m - nA)\right) \frac{1}{\sqrt{2\pi}\sigma} e^{\left(-\frac{(n-\bar{m})^2}{2\sigma^2}\right)}. \quad (16)$$

The MAP estimation is obtained calculating natural logarithm and equating their derivative to zero

$$\ln(p(n|m)) \propto P + \ln\left(\frac{1}{\sqrt{2\pi|\Sigma|}}\right) - \frac{(m - nA)^{T\Sigma^T}(m - nA)}{2} + \ln\left(\frac{1}{\sqrt{2\pi}\sigma}\right) - \frac{(n-\bar{m})^2}{2\sigma^2}, \quad (17)$$

where P refers to the constant of proportionality. Taking derivative of (17):

$$\frac{\partial \ln(p(n|m))}{\partial n} = A^T\Sigma^T(m - nA) + \frac{(n-\bar{m})}{\sigma^2}. \quad (18)$$

The MAP estimate of the noisy pixel is obtained by equating (18) to zero:

$$\hat{n} = \underbrace{\arg\max}\,(p(m|n)) = \frac{-\frac{\bar{m}}{\sigma^2} + A^T\Sigma^T m}{A^T\Sigma^T - \frac{1}{\sigma^2}}. \quad (19)$$

Also, it is known that the despeckling algorithms that use logarithmic transformation of the speckled image converts the multiplicative noise model into additive noise one. Therefore,

(20)

Proc. Of the 3rd International E-Conference on Advances in Engineering, Technology and Management - ICETM 2020

ISBN: 978-1-63248-190-0 DOI: 10.15224/978-1-63248-190-0-13

in [18] has been considered that the converted noise has a Rayleigh distribution described by following:

$$p_n(x|\sigma) = \frac{x}{\sigma^2}\exp\left(-\frac{x^2}{2\sigma^2}\right), \tag{14}$$

where σ represents the scale parameter of distribution.

5) Bilateral Filter

The bilateral filter (BF), originally introduced in [5] for gray scale images has been extended recently to despeckling in [24]. The principal idea of such filtering consists of usage of special weighting, where each pixel value within a sliding window is weighted that is dependent both for the distance to the center and for the difference value to the center. Applying this block, we consider to remove the discontinuities produced by the MAP estimation [25] with the purpose to measure the intensity variations respecting to a central pixel.

One of the principal advantages of the BF is its lower smoothing in comparison with lineal filters and a great edge preservation [26].

$$I_{BF}(a_i) = \exp\left(\frac{\left||f(a_i) - f(a_0)|\right|^2}{2\sigma_R^2}\right). \tag{21}$$

Figure 1 demonstrates a block diagram of the proposed framework, in which, the first step converts the originally affected by speckle noise an image into transformed image with additive noise model using the homomorphic transformation. The second step consists of performing the k-means segmentation where we use patches of size 5×5, which does not generate deformation in the image taking into account that the search is performed through patches and not via pixel by pixel. Then, the patches should be grouped into 3D arrays, which are subjected to calculate the correlation between their patches and estimate the MAP. Here, we use a previous filtering (median filter) in order to obtain approximation of noise-free pixels a priori, according to [31]. All the pixels are replaced by the ones that should be estimated previously. During the fourth step, we perform the exponential transformation and, finally, the bilateral filter is employed along with an edge detector (Sobel operator) to enhance the edge preservation in the whole system.

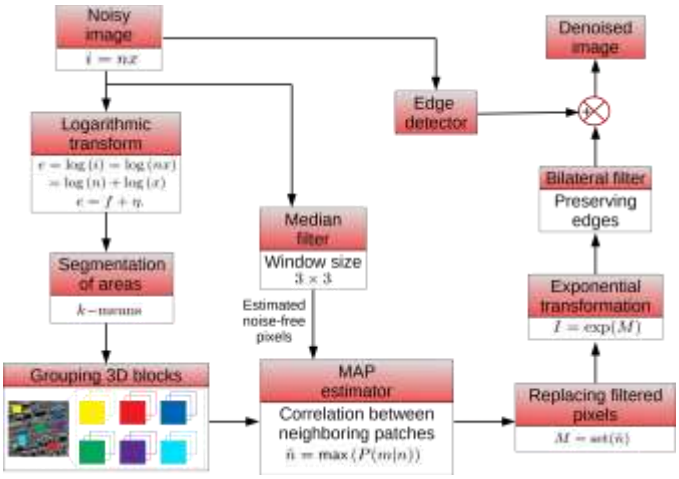

Figure 1. Block diagram of the proposed method.

IV. Denoising Quality Metrics

The evaluation of the proposed algorithm is based on several performance metrics, which compare the denoised(despeckled) image with the original noise-free image [27]. The metrics used for evaluation in this work are listed below.

1) Peak Signal to Noise Ratio

The Peak Signal to Noise Ratio (PSNR) [28] is defined as the ratio between the maximum power that can be presented in an image and the power of the noise affecting this image. For a given noise-free image P and denoised image Q, both of size $M \times M$, the PSNR of Q is calculated as:

$$\mathrm{PSNR}(P,Q) = 10\log_{10}\left(\frac{255^2}{\mathrm{MSE}}\right), \tag{22}$$

where

$$\mathrm{MSE} = \frac{1}{MN}\sum_{i=1}^{M}\sum_{j=1}^{N}\left(P_{i,j} - Q_{i,j}\right)^2. \tag{23}$$

A high value of PSNR denotes a better denoised image.

2) Edge Preservation Index

The Edge Preservation Index (EPI) [29] indicates the amount of edges that is kept in the denoised image. This is important in medical image denoising since the presence of lesion trends to remove edges. The EPI between noise-free image P and denoised image Q is defined as:

$$\mathrm{EPI}(P,Q) = \frac{\sum(\Delta P - \mu_{\Delta P})(\Delta Q - \mu_{\Delta Q})}{\sqrt{\sum(\Delta P - \mu_{\Delta P})^2(\Delta Q - \mu_{\Delta Q})^2}}, \tag{24}$$

Proc. Of the 3rd International E-Conference on Advances in Engineering, Technology and Management - ICETM 2020

ISBN: 978-1-63248-190-0 DOI: 10.15224/978-1-63248-190-0-13

Where ΔP and ΔQ represents the high pass filtered images of P and Q, respectively; and $\mu_{\Delta P}$ and $\mu_{\Delta Q}$ are the mean, respectively. The filter used is a simple 3×3 spatial domain high pass filter H, such as:

$$H_{i,j} = \begin{cases} 1, & \text{for } i,j = 1,2,3; i,j \neq 2 \\ -\sum_{i,j=1;i=j\neq 2}^{3} H_{i,j}, & \text{for } i = j = 2. \end{cases} \quad (25)$$

EPI value extends between $[0,1]$. Closer to 1 means the better denoised image (the edges are preserved well during denoised process).

3) Structural Similarity Index

The Structural Similarity Index Measure (SSIM) [30] indicates how much the denoised image matches with the original image. It is calculated as:

$$\text{SSIM}(P,Q) = \frac{(2\mu_P\mu_Q + c_1)(2\sigma_{PQ} + c_2)}{(\mu_P^2 + \mu_Q^2 + c_1)(\sigma_P^2 + \sigma_Q^2 + c_2)}, \quad (26)$$

where P and Q represent the original image and the denoised image, respectively; μ_P and μ_Q are the mean and σ_P and σ_Q represent the standard deviation of P and Q, respectively; σ_{PQ} is the covariance of P and Q; $c_1 = (p_1 K)^2$ and $c_2 = (p_2 K)^2$ are two constant to avoid division with zero, where K is the dynamic range of the pixel values given by $2^{(\text{bit-per-pixel})} - 1$, $p_1 = 0.01$ and $p_2 = 0.03$. SSIM varies from $[-1,1]$. The best value is indicated by 1.

v. Experimental Results

In this section, we report the experimental results on images obtained from a database. Results were obtained through visual subjective inspection and quantitative analysis, where the proposed method is compared with other state-of-art methods. Tab. 1 presents the comparison of our experimental results with principal state-of-art technique applied on databases from SAR images and US images [31]. The noise was introduced in the images by multiplying with a random Gaussian value, which is denoted by σ (standard deviation).

Table 1. Specifications of filters used for comparison.

S. no.	State-of-art methods			
	Method	***Ref.***	***Experiment***	***Category***
Method 1	Frost	[32]	Window size 5×5	Spatial filter
Method 2	Lee	[33]	Window size 3×3	Spatial adaptive filter.
Method 3	BM3D-DCT	[34]	Eigen value threshold $\lambda = 49$	Hybrid
Method 4	t-SVD	[35]	Decomposition level $j = 5$	Hybrid
Method 4	MSRAD	[31]	$\lambda = 0.0005$, $\gamma = 2.0$	Hybrid

To make the results more convincing, the proposed framework is compared with better state-of-art techniques from different categories and the classical filters for speckle reduction (Lee and Frost). The Fig. 2 shows the filtered image and its error images. The Tab. 2 shows the comparison of PSNR, SSIM and EPI criteria values, respectively when different techniques were applied in the image S-01.

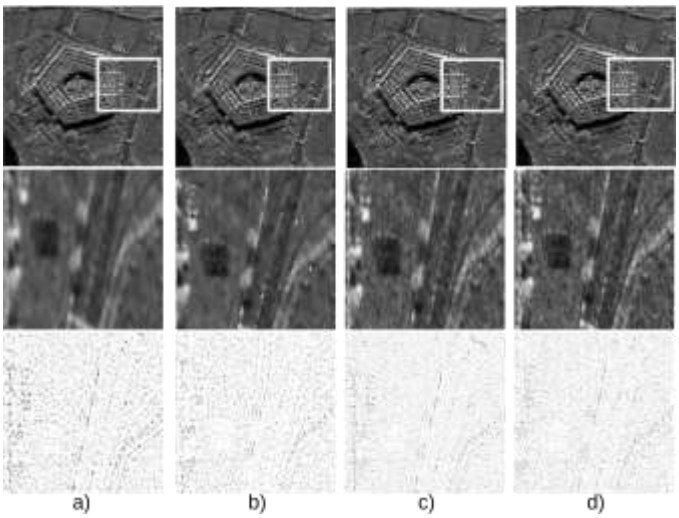

Figure 2. Image S-01 with σ=0.04. First row: filtered image; second row: zoomed filtered image; third row: zoomed error image. a) method 2, b) method 3, c) method 4 and d) proposed method.

Table 2. Criteria values for image S-02

Method	Noise level (σ)			
	0.02	**0.04**	**0.08**	**0.1**
PSNR				
1	28.26	27.76	26.52	24.78
2	29.54	28.61	28.04	28.20
3	30.26	29.50	29.01	26.81
4	30.74	30.15	29.58	28.52
5	31.21	31.18	30.84	31.10
Proposed	31.57	31.56	32.98	32.38
SSIM				
1	0.9525	0.8932	0.8435	0.7854
2	0.9630	0.9016	0.8492	0.7865
3	0.9682	0.9046	0.8549	0.7732
4	0.9723	0.9132	0.8587	0.7798
5	0.9767	0.9159	0.8715	0.7817
Proposed	0.9815	0.9345	0.8845	0.8165
EPI				
1	0.9525	0.9224	0.9119	0.9023
2	0.9630	0.9455	0.9325	0.9214

ISBN: 978-1-63248-190-0 DOI: 10.15224/978-1-63248-190-0-13

Method	Noise level (σ)			
	0.02	**0.04**	**0.08**	**0.1**
3	0.9548	0.9351	0.9326	0.9189
4	0.9658	0.9409	0.9408	0.9204
5	0.9522	0.9478	0.9419	0.9227
Proposed	0.9668	0.9547	0.9442	0.9375

The Fig. 3 shows the filtered images and their error images. The Tab. 3 shows the comparison of PSNR, SSIM and EPI criteria values, respectively, when different techniques were applied in the image U-01.

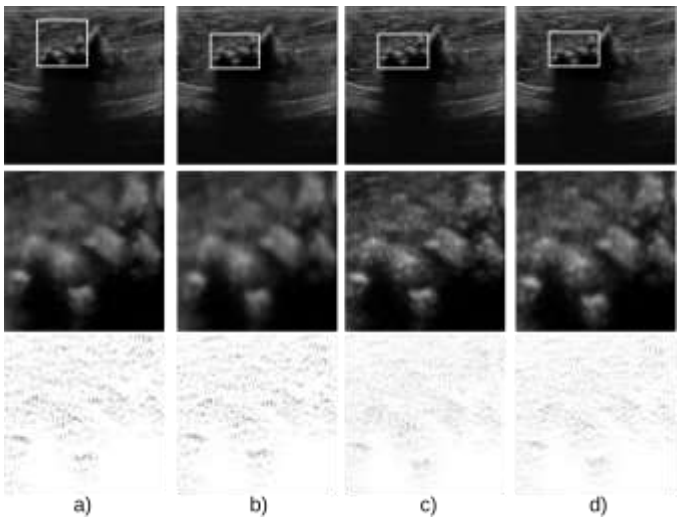

Figure 3. Image U01- with σ=0.04. First row: filtered image; second row: zoomed filtered image; third row: zoomed error image. a) method 2, b) method 3, c) method 4 and d) proposed method.

Table 3. Criteria values for image U-02.

Method	Noise level (σ)			
	0.02	**0.04**	**0.08**	**0.1**
PSNR				
1	25.31	24.46	21.86	21.19
2	25.47	24.12	22.54	21.23
3	25.57	24.01	22.67	21.75
4	25.43	23.49	23.24	22.69
5	25.39	24.00	23.58	22.85
Proposed	26.47	24.65	23.32	23.17
SSIM				
1	0.8911	0.8718	0.8547	0.8336
2	0.8942	0.8819	0.8718	0.8436
3	0.9002	0.8888	0.8811	0.8539
4	0.8922	0.8904	0.8852	0.8616
5	0.9145	0.8975	0.8821	0.8718
Proposed	0.9146	0.9002	0.8901	0.8841
EPI				
1	0.8496	0.8204	0.8086	0.8011
2	0.8614	0.8481	0.8296	0.8184
3	0.8495	0.8406	0.8396	0.8289
4	0.8641	0.8547	0.8414	0.8328
5	0.8698	0.8591	0.8503	0.8400
Proposed	0.8710	0.8616	0.8573	0.8437

VI. Discussion

The performance of the proposed method is compared with the despeckling methods shown in Tab. 1, also using zoomed part of the images. One can see that the methods 1 and 2 do not produce an effective amount in speckle reduction. This can be seen observing the noise detailed components that were not suppressed well. In opposite, the methods 3, 4, 5 and the proposed framework demonstrated a good despeckling performance. Additionally, the edges can be viewed much more well preserved. This fact is important in different remote sensing applications where, after despeckling of SAR images, the objects of interest are usually characterized by the edges that play a crucial role in detection. The same performance is important in medical imaging, where the images are used for classification or diagnostics, for example, in detection of malignant cells.

As it is known, that the human eye is not merely enough to evaluate the despeckling methods because the image has tiny details, which are difficult to distinguish via the human perception system. Therefore, the use of the metrics presented previously helps to measure the performance of different despeckling methods. As one can see, the proposed method has the highest values for PSNR, SSIM and EPI criteria, which indicates that designed framework appears to demonstrate a good speckle reduction and high edge preservation. Considering the method 1 and 2 as the classical filters for speckle suppression, one can see that they tend to get lower values. In opposite, the methods 3,4 and 5 present sufficiently good criteria values.

VII. Conclusion

This study presents a novel despeckling approach that can be used for SAR and US images via incorporating the statistical properties of these images. To develop this framework, we have considered the statistical properties of the speckle noise in the images. Our scheme employs statistical method to calculate the correlation between a group of similar

ISBN: 978-1-63248-190-0 DOI: 10.15224/978-1-63248-190-0-13

patches in the 3D arrays formed. Using this correlation, the MAP estimation in the 3D arrays and applying the bilateral filtering, novel framework appears to demonstrate sufficiently good despeckling ability and edge preservation performance of the images.

Experimental results performed in different images from databases have confirmed the highest objective criteria values for PSNR, SSIM, and EPI in comparison with the state-of-art methods.

References

[1] H. Arsenault, M. Levesque, "Combined homomorphic and local-statistics processing for restoration of images degraded by signal dependent noise", Appl. Opt., vol. 13, no. 6, pp. 845–850, 1984.

[2] I. Daubechies. "Orthonormal bases for compactly supported wavelets", Commun. Pure Appl. Math., vol. 41, no. 7, pp. 909–996, 1988.

[3] S. Mallat, "A theory for multiresolution signal decomposition: The wavelet representation", IEEE Trans. Anal. Mach. Intell., vol. PAMI-11, no. 7, pp. 674–693, 1989.

[4] F. Guan, P. Tons, S. Ge, L. Zhao, "Anisotropic diffusion filtering for ultrasound speckle reduction", Science China Technological Sciences, vol. 57, no. 3, pp. 607–614, 2014.

[5] C. Tomasi, R. Manduchi, "Bilateral filtering for gray and color images", Sixth International Conference on Computer Vision, IEEE, pp. 839–846, 1998.

[6] S. Balocco, C. Gatta, O. Pujol, J. Mauri, P. Radeva: "SRBF: Speckle reducing bilateral filtering", Ultrasound in Medicine and Biology, vol. 36, no. 3, pp. 1353–1363, 2010.

[7] J. Zhang, G. Lin, L. Wu, Y. Cheng, "Speckle filtering of medical ultrasonic images using wavelet and guided filter", Ultrasonics, vol. 65, pp. 177–193, 2016.

[8] Y. Yu, S.T. Acton, "Speckle reducing anisotropcj diffusion", IEEE Transacntions on Image Processing, vol. 11, no. 11, pp. 1260–1270, 2002.

[9] N. Damodaran, S. Ramamurthy, S. Velusamy, G.K. Manicakam, "Speckle noise reduction in ultrasound biomedical B-scan images using descrete topological derivative", Ultrasound in Medicine and Biology, vol. 38, no. 2, pp. 276–286, 2012.

[10] K. Krissian, C.F. Kikinis, K.G. Vosburgh, "Oriented speckle reducing anisotropic diffusion", IEEE Transactions on Image Processing, vol. 16, no. 5, pp. 1412–1424, 2007.

[11] P. Coupé, P. Hellier, C. Kervann, C. Barillot, "Nonlocal means-based speckle filtering for ultrasound images", IEEE Transactions on Image Processing, vol. 18, no. 10, pp. 2221–2229, 2009.

[12] J.S. Lee, "Digital image enhancement and noise filtering by use of local statistics", IEEE, Transactions on Pattern Analysis and Machine Intelligence, vol. 2, pp. 165–168, 1980.

[13] D. Donoho, J.M. Johnstone, "Idel spatial adaptation by wavelet shrinkage", Biometrika, vol. 81, no. 3, pp. 425–455, 1994.

[14] G. Andria, F. Attivissimo, G. Cavone, N. Giaquinto, A. Lanzolla, "Linear filtering of 2-D wavelet coefficients for denoising ultrasound medical images", Measurement, vol. 45, no. 7, pp. 1792–1800, 2012.

[15] K. Dabov, A. Foi, K. Katkovnik, K. Egiazariam, "BM3D image denoising with shaped-adaptive principal component analysis", SPARS'09–Signal processing with adaptive sparse structured representations, 2009.

[16] M.F. Insana, K.J. Myers, L.W. Grossman, "Signal modeling for tissue characterization" Handbook of medical imaging, vol. 2, Bellingha, WA: SPIE, 2008.

[17] G. Parry, J. Dainty, "Speckle reduction with improved resolution in ultrasound images" IEEE Transactions on Sonics and Ultrasounds, vol. 32, no. 4, pp. 537–543, 1985.

[18] C.B. Burckhardt, "Speckle in ultrasound B-mode scans ", IEEE Transactions on Sonics and Ultrasonics, vol. 25, no. 1, pp. 1–6, 1978.

[19] R.F. Wagner, S.W. Smith, J.M. Sandrick, H. Lopez, "Statistics of speckle in ultrasound B-scans", IEEE Transactions on Sonics and Ultrasnoics, vol. 30, no. 3, pp. 165–163, 1983.

[20] E. Jakeman, R. Tough, "Generalized K distribution: A statistical model for weak scattering", JOSA A, vol. 4, no. 9, pp. 1764–1772, 1987.

[21] L. Weng, J.M. Reid, P.M. Shankar, K. Soetano, "Ultrasound speckle analysis based on the K distribution", The Journal of the Acoustical Society of America, vol. 89, no. 6, pp. 2992–2995, 1991.

[22] J. Tian, L. Chen, "Image despeckling using a non-parametric statistical model of wavelet coefficients", Biomedical Signal Processing and Control, vol. 6, no. 4, pp. 432–437, 2011.

[23] X. Zong, A.F. Laine, E.A. Geiser, "Speckle reduction and contrast enhancement of echocardiograms via multiscale nonlinear processing", IEEE Transactions on Medical Imaging, vol. 17, no. 4, pp. 532–540.

[24] W.G. Zhang, Q. Zhang, C.S. Yang, "Improved bilateral filtering for SAR image despeckling", Electronics Letters, vol. 47, no. 4, pp. 286–288, 2011.

[25] H. Winnermoller, S. Olsen, "Real-time video abstraction" In, ACM SIGGRAPH, vol. 25, pp. 1221, 2011.

[26] H. Heygster, "Rank filters in digital image processing", Comp, and Im. Process., vol. 19, pp. 148–168, 2004.

[27] N. Biradar, M. Dewal, Rohit, S. Gowre, Y. Gundg, "Blind source parameters for performance evaluation of despeckling filters" Int. J. Biomed. Imag

[28] J. Zhang, G. r based despec l Signal Proces

[29] Z. Farook, F. a nonlinear mu vol.6, no. 6, p

[30] Z. Wang, A. y assessment fi Image, Proces

[31] V. Sameera, a sequence of Imaging, pp.

[32] V.S. Frost, J.A. Stiles, K.S. Shanmugan, J.C. Holtzman, "A model for radar images and its applications to adaptive digital filtering of multiplicative noise", IEEE Transactions on Pattern Analysis and Machine Intelligence, vol. 2, pp. 157–166.

[33] J.S. Lee, "Digital image enhancement and noise filtering by use of local statistics", IEEE Transactions on Pattern Analysis and Machine Intelligence, vol. 2, pp. 165–168.

[34] A. Palacios-Enriquez, V. Ponomaryov, R. Reyes-Reyes, S. Sadovnichy, "Sparse technique for Images corrupted by mixed Gaussian-impulsive noise", Circuits Systems and Signal Processing, 2018.

[35] V. Sameera, S. Sudhish, K. Sudeep, "Despeckling of 3D ultrasound image using tensor low rank approximation", Biomedical Signal Processing and Control, vol. 54, 2019.

Rogelio Reyes-Reyes received the B. Sc. degree in communications and electronics engineering from the Escuela Superior de Ingenieria Mecanica y Electrica (ESIME) and the M. Sc. and Ph. D. degrees in electronics and communications from the Graduate Section of ESIME Culhuacan of the Instituto Politecnico Nacional (IPN) Mexico. His main researches lines are vide and image processing, network security and related fields.

ISBN: 978-1-63248-190-0 DOI: 10.15224/978-1-63248-190-0-13

About Author (s):

Gibran Aranda-Bojorges received the B. Sc. degree in bionics engineering from the Unidad Profesional Intedisciplinaria en Ingenieria y Tecnologias Avanzadas (UPIITA) and the M. Sc. degree from the Centro de Innovacion y Desarrollo Tecnologico en Computo (CIDETEC) of the Instituto Politecnico Nacional (IPN), Mexico. His main research lines are signal, image and video processing, artificial intelligence and related fields.

Volodymyr Ponomaryov: Ph.D. (1974), D. Sci. (1981), Full Professor (1984). He is working as Professor at Instituto Politecnico Nacional (Mexico-city). Main research activity: signal/image processing, real time filtering, remote sensing, etc. He is author more than 250 international scientific papers, 350 conference papers, and also 23 patents of exUSSR, Russia and Mexico, and several scientific books.